THE JOURNAL OF BIOLOGICAL CHEMISTRY
Vol. 279, No. 11, Issue of March 12, pp. 10692–10701, 2004

Printed in U.S.A.

The Single Dynamin-like Protein of *Trypanosoma brucei* Regulates Mitochondrial Division and Is Not Required for Endocytosis*

Received for publication, November 6, 2003, and in revised form, December 5, 2003
Published, JBC Papers in Press, December 11, 2003, DOI 10.1074/jbc.M312178200

Gareth W. Morgan, David Goulding, and Mark C. Field‡

From the Wellcome Trust Laboratories for Molecular Parasitology, Department of Biological Sciences, Imperial College, Exhibition Road, London SW7 2AY, United Kingdom

Members of the evolutionarily conserved dynamin-related GTPase family mediate numerous cellular membrane remodeling events. Dynamin family functions include the scission of clathrin-coated pits from the plasma membrane, mitochondrial fission, and chloroplast division. Here we report that the divergent eukaryote *Trypanosoma brucei* possesses a single dynamin family gene, which we have designated *TbDLP*. Furthermore, a single dynamin family gene is also found in the *Leishmania major* and *Trypanosoma vivax* genomes, indicating that this is a conserved feature among the kinetoplastida. TbDLP is most homologous to the DMN/DRP family of dynamin-like proteins. Indirect immunofluorescence microscopy reveals that TbDLP is distributed in punctate structures within the cell that partially co-localize with the mitochondrion when labeled with MitoTracker. To define TbDLP function, we have used RNA interference to silence the *TbDLP* gene. Reduction of TbDLP protein levels causes a profound alteration in mitochondrial morphology without affecting the structure of other membrane-bound compartments, including the endocytic and exocytic apparatus. The mitochondrial profiles present in wild type trypanosomes fuse and collapse in the mutant cells, and by electron microscopy the mitochondria are found to contain an accumulation of constriction sites. These findings demonstrate TbDLP functions in division of the mitochondrial membrane. Most significantly, as TbDLP is the sole member of the dynamin family in this organism, scission of clathrin-coated pits involved in protein trafficking through the highly active endocytic system in trypanosomes must function in the absence of dynamin. The evolutionary implications of these findings are discussed.

The kinetoplastida protozoa of the *Trypanosoma brucei* group are significant as one of the earliest diverging eukaryotic lineages that contain a single mitochondrion (1). Given their extreme evolutionary distance, estimated at a divergence time of ~3 billion years from the crown eukaryotes, it is not unexpected that these organisms display many unusual biological features. One example is a unique configuration of the mitochondrial genome, the kinetoplast DNA, which is composed of several thousand DNA circles catenated into a single network (2). This network is condensed into a disk-shaped structure in the matrix of the single mitochondrion of the cell and is structurally linked to the flagellar basal bodies through a *trans*-membrane complex (3, 4). The *T. brucei* life cycle alternates between the mammalian host stages and insect vector stages, which are coupled to extensive alterations in morphology and metabolism (5, 6). In particular, the mitochondrion undergoes extensive remodeling at the structural and biochemical level (7). Procyclic trypanosomes (PCF)[1] maintain a developed mitochondrion with abundant cristae, whereas in the replicative slender bloodstream form (BSF), the mitochondrion is greatly reduced with scarcely any cristae. The bloodstream form lacks cytochromes, several key enzymes of the Krebs cycle, and is incapable of full oxidative phosphorylation (8). This remodeling reflects fundamental differences in the energy metabolism between the two life cycle stages (7, 9).

Dynamin was initially identified as a protein that assembled into rings at the necks of nascent clathrin-coated vesicles (CCVs) during their liberation from the plasma membrane in higher eukaryotes (10, 11). Dynamin is a GTPase containing five distinct domains as follows: an N-terminal domain with a tripartite GTP-binding motif (12); a middle domain with a potential role in self-assembly; a pleckstrin homology domain, which has membrane binding properties (13); a coiled coil region that constitutes a GTPase effector domain (14); and a C-terminal proline/arginine-rich domain (15) required for self-assembly and containing several Src homology 3-binding sites for binding interacting partners (Fig. 1*A*) (11, 16). Numerous dynamin-like proteins (DLPs) have also been identified, which are quite diverse with regard to sequence and to biological function but share critical roles in membrane remodeling (16, 17).

Sequence homology within the dynamin family is primarily restricted to the GTPase and middle domains. DLPs generally lack the pleckstrin homology domain and proline/arginine-rich domains but contain several insertions relative to dynamin (Fig. 1*A*) (17). The most comprehensively characterized DLPs are the three encoded by the *Saccharomyces cerevisiae* genome, *VPS1*, *DNM1,* and *MGM*. Vps1p is associated with the Golgi complex, is required for proper sorting of proteins to the yeast vacuole (18), and has also been implicated in peroxisome abundance and inheritance (19). Dnm1p is mostly cytosolic and functions primarily in the maintenance of yeast mitochondrial

* This work was supported by a program grant from the Wellcome Trust (to M. C. F.). The costs of publication of this article were defrayed in part by the payment of page charges. This article must therefore be hereby marked "*advertisement*" in accordance with 18 U.S.C. Section 1734 solely to indicate this fact.

The nucleotide sequence(s) reported in this paper has been submitted to the GenBank™/EBI Data Bank with accession number(s) AF156167.

‡ To whom correspondence should be addressed. Tel.: 0044-020-7594-5277; E-mail: mfield@ic.ac.uk.

[1] The abbreviations used are: PCF, procyclic form; BSF, bloodstream form; BiP, binding protein; CCV, clathrin coated vesicles; CHC, clathrin heavy chain; DLP, dynamin-like protein; DRP dynamin-related protein; RNAi, RNA interference; ORF, open reading frame; PFA, paraformaldehyde; ConA, concanavalin A; PBS, phosphate-buffered saline; ER, endoplasmic reticulum; GAPDH, glyceraldehyde-3-phosphate dehydrogenase; DAPI, 4,6-diamidino-2-phenylindole.

network morphology (20, 21). Mgm1p is located in the intermitochondria space and is required for maintenance of fusion-competent mitochondria (22).

The exact mechanism underpinning the function of dynamin in membrane remodeling is the subject of much debate (23). Dynamins are able to spontaneously self-assemble *in vitro* into rings and spirals when provided with a suitable lipid template. Upon the addition of GTP, the dynamin rings alter pitch and constrict (24, 25). This observation leads to the hypothesis that dynamin is a force-generating mechano-enzyme. Alternatively, analysis of the dynamin GTPase effector domain leads to a second model of dynamin action suggesting that the protein may function as a classical regulatory GTPase that recruits and/or activates additional effector molecules responsible for membrane scission (26).

Trypanosomes possess a highly active endocytic system capable of carrying out the clathrin-dependent recycling of plasma membrane proteins (27, 28). Here we report the identification of a trypanosomal DLP (*TbDLP*) with high homology to yeast dynamin-like proteins VPS1 and DNM1. Data base interrogation indicates that kinetoplastid protozoa are unique in having a single DLP encoded in their genome. Our data demonstrate that TbDLP, like yeast DNM1 and MGM, functions in the regulation of mitochondrial membrane division. Hence, trypanosomes are able to carry out clathrin-mediated endocytosis in the absence of a dynamin-like GTPase.

EXPERIMENTAL PROCEDURES

Trypanosome Cells and Culture—PCF and BSF cells, strain 427, were maintained in SDM79 and HMI9 media, respectively, as described previously (29). The inducible cell lines PCF 29-13 and BSF 90-13 were obtained from George Cross (Rockefeller University) and maintained as described (30).

Data Base Searches, DNA Cloning, and Manipulation—We identified a trypanosomal EST fragment (GenBank™ accession number T26974) most homologous to yeast VPS1 from a search of the TIGR *T. brucei* Genome Project (www.tigr.org/tdb/mdb/tbdb/) by using the BLAST algorithm (31). A DNA fragment was PCR-amplified from *T. brucei* genomic DNA using specific primers (5′-TGGATTCCTTCCTTCTCGTGGT-3′ and 5′-AGTGTCCAAGCACTTCCGTT-3′) designed against the T26974 EST and subcloned. This fragment was radiolabeled and used to probe a *T. brucei* λFIX genomic library by filter hybridization (32) to obtain the entire trypanosomal dynamin-like protein (*TbDLP*) ORF. The *TbDLP* sequence was submitted to GenBank™ (GenBank™ accession number AF156167). The entire *TbDLP* ORF has also been independently identified by the trypanosomal genome projects at the Sanger Institute (Tb03.48K5.290 and Tb03.48K5.360) and TIGR (62.m00222 and 62.m00230), which is present as two copies.

Generation of Constructs—PCR was performed with *Pfu* polymerase (Stratagene, La Jolla, CA). PCR products were subcloned using the PCR-Script Amp cloning kit (Stratagene, La Jolla, CA) and sequenced with the "BigDye" terminator chemistry version 3.0 (Applied Biosystems, Foster City, CA) and a semiautomated sequencer (ABI 377; PerkinElmer Life Sciences), according to the manufacturer's instructions.

Bioinformatics—Sequence comparisons and phylogenetic tree analyses were performed using the ClustalX multiple alignment program (33), and phylogenetic reconstruction was done using PAUP release 4.0* (Phylogenetic Analysis Using Parsimony) (34) with at least 1,000 bootstrap replications. GenBank™ accession numbers for the sequences used in these analyses are given in the legend to Fig. 1.

RNA Interference—An RNAi construct was made using the vector $p2T7^{Ti}$ (35), which allows for stable tetracycline-inducible expression of double-stranded RNA from a T7 promoter in *T. brucei* 29-13 procyclic and BSF Lister 427 bloodstream form cell lines. A 475-bp HindIII/SacI TbDLP fragment was subcloned into the corresponding sites of $p2T7^{Ti}$.

Antibody Production—TbDLP antiserum was generated against an N-terminal peptide (residues 12–25, CHDAFANVKMNIKLN which includes an N-terminal C, not present in the native sequence, for coupling) in rabbits and mice. Antibodies were affinity-purified on antigen immobilized on cyanogen bromide-activated Sepharose 4B (Amersham Biosciences) by using standard procedures (36).

Immunofluorescence Microscopy—Cells were washed in PBS and fixed in 3% paraformaldehyde (PFA) in PBS, pH 7.5, for 10 min (BSF) or 1 h (PCF) on ice as described previously (27). All further manipulations were performed at room temperature. Mitochondrial morphology was assessed by incubating cultures in MitoTracker Green FM/Red CMXRos (Molecular Probes, Eugene, OR) for 5 min prior to live cell imaging or fixation. Concanavalin A (ConA) uptake was performed as described previously (37). Briefly, ConA was bound by incubation of cells in serum-free medium supplemented with 5 μg/ml fluorescein ConA (Vector Laboratories, Burlingame, CA) at 4 °C for 30 min before washing and direct transfer to 37 °C for internalization. Cells were examined using a Nikon ECLIPSE E600 epifluorescence microscope equipped with a Nikon digital DMX 1200 camera (Nikon Europe B.V., AE Badhoev, The Netherlands). Digital images were captured using Nikon ACT-1 software and assembled using Adobe Photoshop (Adobe Systems, Inc., San Jose, CA).

Western Blots—1×10^7 cells per lane were electrophoresed on 12% SDS-polyacrylamide gels and blotted onto Hybond ECL nitrocellulose membrane (Amersham Biosciences) by wet transfer. Filters were processed as described (29).

Electron Microscopy—For transmission EM, cells were fixed in suspension by adding chilled 5% glutaraldehyde and 8% PFA in PBS in a 1:1 ratio to the growth medium containing trypanosomes. Cells were pelleted and incubated with fresh fixative for a further 50 min. The pellet was rinsed in 0.1 M sodium cacodylate and post-fixed in 1% osmium tetroxide for 1 h. After rinsing, cells were dehydrated in an ethanol series, adding 1% uranyl acetate at the 30% stage, followed by propylene oxide, and then embedded in Epon/Araldite. Sections were cut on a Leica Ultracut T ultramicrotome, contrasted with uranyl acetate and lead citrate. For cryosectioning, cells were fixed in suspension by adding chilled 0.4% glutaraldehyde and 8% PFA in PBS in a 1:1 ratio to the growth medium containing trypanosomes to give final dilutions of 0.2% glutaraldehyde and 4% PFA. Cells were fixed for 10 min on ice and centrifuged, and the supernatant was replaced for fresh fixative for a further 50 min on ice to fix the pellet. The cells were then rinsed three times in cold PBS for 15 min and then infused with freshly prepared 2.3 M sucrose in cold PBS between 8 h and overnight prior to freezing in liquid nitrogen and storage in a refrigerator. Thin sections of frozen cells were cut and processed for immunogold labeling, after free aldehyde groups were blocked by incubation with 0.05 M glycine for 5 min. The sections were then incubated with the TbDLP antibody, which was visualized using protein A-gold 10-nm conjugates. All sections were examined on a Philips CM100 transmission electron microscope.

RESULTS

Identification of a Trypanosomal Dynamin-like Protein—Interrogation of the *T. brucei* genome project data bases with a collection of dynamin and dynamin-like protein sequences by BLAST identified an EST fragment (GenBank™ accession number T26974) with homology to the yeast dynamin-like protein VPS1 (18). Screening a λFIX *T. brucei* library allowed the isolation of a genomic clone containing the corresponding full-length open reading frame (1983 bp) that encoded a 661-amino acid polypeptide with a predicted molecular mass of 73.3 kDa. The entire TbDLP ORF has also been sequenced by the trypanosomal genome projects at Wellcome Trust Sanger Institute (Tb03.48K5.290 and Tb03.48K5.360) and the Institute for Genomic Research (62.m00222 and 62.m00230). The protein contains structural domains present in other dynamin family members including the dynamin catalytic family motif (pfam00350, residues 2–213), dynamin 2 central region (pfam01031, residues 214–498), and the dynamin GTPase effector domain (pfam02212, residues 571–635). A schematic representation of the protein domains of the dynamin protein family is shown in Fig. 1*A*. The nearest *TbDLP* homologue identified using BLAST is *Dictyostelium discoideum* DymA (38), which exhibits ~65% homology and ~49% similarity. As shown in Fig. 1*B*, *TbDLP* (like the ScMgm protein) lacks inserts in the N-terminal GTPase domain (*underlined*) that occur in ScVps1 and ScDnm1 DLPs (17).

TbDLP is single copy gene by Southern blot analysis, and no related genes could be detected under low stringency conditions (data not shown). This was unexpected as most organisms investigated to date have at least two DLP family members in their genome. To verify this finding, we extensively searched

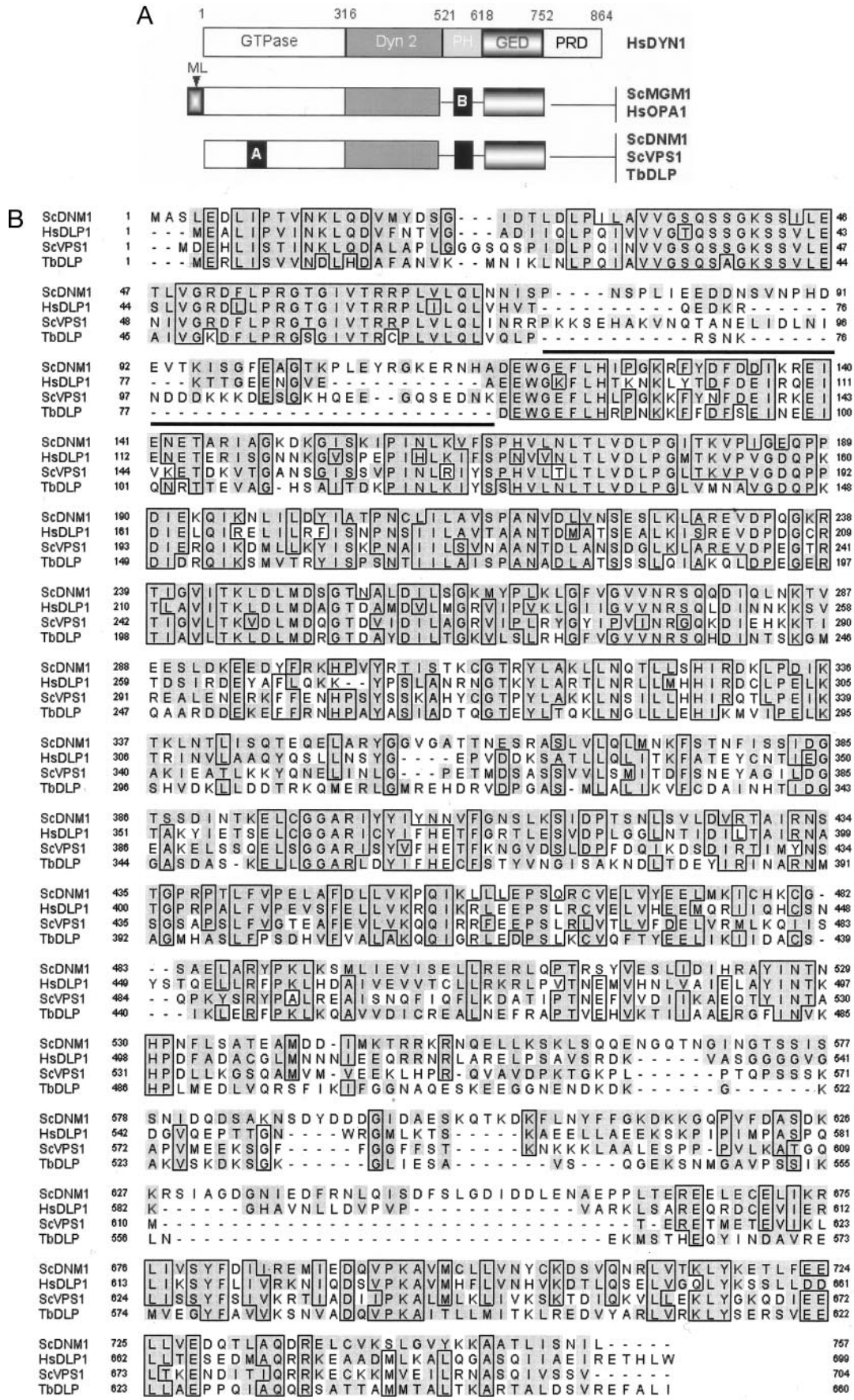

FIG. 1. **Homology between TbDLP and the dynamin family.** *A*, schematic representation of the protein domains of dynamin homologues. Human dynamin 1 (*HsDYN1*) is involved in endocytosis and is the prototype member of the family; it possesses a GTPase domain for GTP binding and hydrolysis, a middle conserved domain (*Dyn_2*), a pleckstrin homology (*PH*) domain, a GTPase effector domain (*GED*) for self-assembly, and

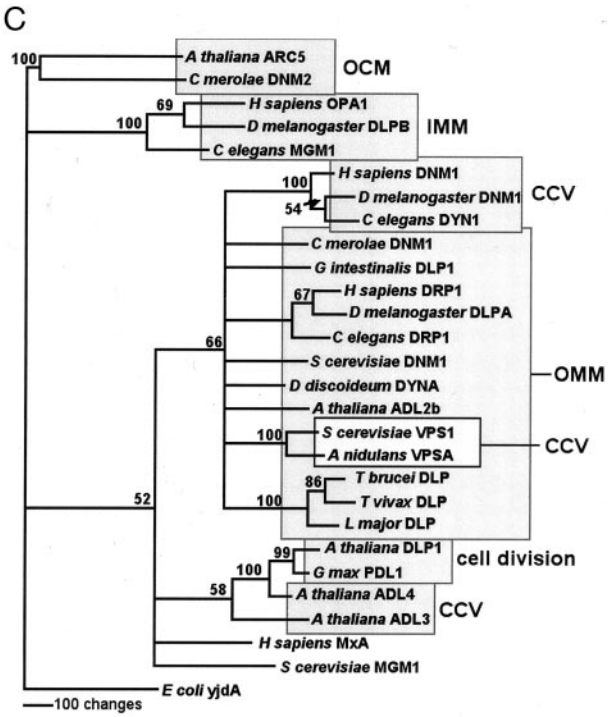

FIG. 1—*continued*

all available *T. brucei* genomic EST and GSS data bases with both the TbDLP sequence and the dynamin family sequences utilized in the original search, but we failed to identify any further DLP homologues in *T. brucei*. By contrast, we recovered full-length sequence homologues of *TbDLP* in the genome data bases of related organisms, specifically *Leishmania major* (CHR29_tmp.127c) and *Trypanosoma vivax* (Tviv273e05.q1k, Tviv604h09.p1k, Tviv143a08.q1k, Tviv120g02.q1k, and Tviv58h12.p1k). These organisms do not contain additional DLP sequences, and hence possession of a single DLP appears to be a widespread feature among the kinetoplastida.

Phylogenetic reconstruction using PAUP (34) demonstrated that the dynamin protein family forms several discrete clades (Fig. 1*C*). Importantly, these clades contain functionally related dynamin family members and are defined by *Arabidopsis thaliana* ARC5 and *Cyanidioschyzon merolae* DNM2, which function in outer chloroplast membrane division; human OPA1, *Drosophila* DLPB, and *Caenorhabditis elegans* MGM1, which function in remodeling of the inner mitochondrial membrane; numerous dynamins required for the release of clathrin-coated vesicles (CCVs), higher plant proteins involved in formation of the cell plate during division (*A. thaliana* DLP1/*G. max* PDL1), and a separate clade functioning in CCV release (*A. thaliana* DLP3/4). Additional members of the dynamin family include the Mx family of proteins involved in vertebrate response to viral infection and the yeast MGM1 protein required for mitochondrial genome maintenance and morphology of the inner mitochondrial membrane. The tree was generated using the *Escherichia coli* protein YjdA, which shares characteristics of dynamin family members as outgroup (17).

Typanosomal DLP segregates with the largest group of DLPs that contains sequences from metazoans, fungi, algae, and protozoa involved in the division of the outer mitochondrial membrane, suggesting a role in this process for TbDLP. This group also contains the yeast protein VPS1 that functions in vacuolar sorting and peroxisome biogenesis. Given the early divergence of trypanosomatids during eukaryotic evolution, the presence of dynamin-like proteins in this lineage indicates kinetoplastid dynamins predate eukaryotic speciation and suggests that this role may represent the original function for the dynamin family of proteins.

Characterization of TbDLP Expression and Specific Antibodies—Northern blot analysis of BSF and PCF demonstrates *TbDLP* mRNA is expressed as a single transcript of 2.1 kb in both life cycle stages (data not shown). To characterize the TbDLP protein, we generated antisera in rabbits and mice against the N-terminal peptide residues 12–25, CHDAFANVKMNIKLN, which following affinity purification were characterized in detail and yielded identical data. By Western blot analysis of BSF and PCF lysates, the sera were found to identify a single band of ~73 kDa which is expressed at slightly higher levels in the PCF than the BSF (Fig. 2*A*). Equivalence of loading was confirmed by reprobing the filter with antibody against *T. brucei* BiP, which has been demonstrated previously to be expressed at ~3-fold more in BSF compared with PCF (39).

To determine the subcellular localization of TbDLP, the affinity-purified antibodies were used in immunofluorescence analysis of paraformaldehyde-fixed PCF and BSF (Fig. 2*B*). This analysis localized TbDLP to numerous reticular and punctate peripheral structures within the cell cytoplasm. The merged image of the TbDLP stain and DAPI fluorescence of the PCF and BSF shows a small pool of TbDLP is partially co-localized with the kinetoplast.

TbDLP Is Localized to the Mitochondrion—To determine in more detail the location of TbDLP, and in particular to attempt

a proline-rich domain (*PRD*) at the C terminus. The second structural group, comprising *S. cerevisiae* ScMGM1 and human HsOPA1, is involved in the maintenance of mitochondrial morphology and localizes to the mitochondrial inner membrane via a leader sequence (mitochondrial leader, *ML*). The third group contains yeast ScDNM1, which is required for mitochondrial division, ScVPS1, involved in vesicular transport and TbDLP. TbDLP, like other proteins from this subfamily, lacks a pleckstrin homology and proline-rich domain. DLPs also have an additional insert, annotated as *A* and *B*. Regions of similar sequence are shown with the same *shading*. Amino acid numbering for HsDYN1 is shown at *top*. *B*, sequence alignment of dynamin-like proteins ScDNM1, ScVPS1, HsDLP1, and TbDLP. Conserved residues are *boxed*, and conservative mutations are *shaded*. TbDLP, like the ScMGM proteins, lacks an insert in the N-terminal GTPase domain found in ScVPS and ScDNM DLPs (*underlined*). *C*, phylogenetic analysis demonstrates TbDLP is a member of the mitochondrial dividing dynamin-like protein family. The clades highlighted are as follows: DLPs that function in outer chloroplast membrane (*OCM*); DLPs located in the mitochondrial space involved in modulating the inner mitochondrial membrane (*IMM*); dynamins that participate in vesicular trafficking of clathrin-coated vesicles from the plasma membrane (*CCV*); DLPs that are predominantly involved in outer mitochondrial membrane (*OMM*) fission (this group also contains the yeast proteins involved in CCV traffic), plant DLPs that are involved in cell plate formation (cell division), and release of clathrin-coated vesicles (*CCV*). The more divergent member is the MxA protein that combats viral infection in vertebrates and the yeast MGM protein. GenBank™ accession numbers for the proteins used in this analysis are as follows: *A. thaliana* ARC5 (AAO89221); *C. merolae* DNM2 (AY162473.1), *Homo sapiens* OPA (Z47808), *C. elegans* MGM1 (AB011139), *D. melanogaster* DLPB (NP_610941), *H. sapiens* DNM1 (NM004408), *D. melanogaster* DMN (NP_727910), *C. elegans* DNM1 (AF167982), *S. cerevisiae* DNM1 (L40588), *H. sapiens* Drp1 (AF000430), *D. melanogaster* DLPA (NP_608694), *C. elegans* Drp1 (AF166274), *D. discoideum* DYNA (CAA67983), *C. merolae* DNM1 (AAO23012), *A. thaliana* ADL2b (AB072375), *S. cerevisiae* VPS1 (M33315), *A. nidulans* VPSA (AB074883.1), *Leishmania major* DLP (Sanger CHR29_tmp.127c), *T. brucei* DLP (AF156167.1; Sanger 62.m00230 and 62.m00222), *T. vivax* DLP (Tviv273e05.q1k, Tviv604h09.p1k, Tviv143a08.q1k, Tviv120g02.q1k, and Tviv58h12.p1k), *Giardia intestinalis* VPSA (AAL87662), *A. thaliana* ADL1 L36939, *Glycine max* (U25547), *A. thaliana* ADL3 (AB026987), *A. thaliana* ADL6 (AF180732), *H. sapiens* MxA (P20591), and *S. cerevisiae* MGM1 (X62834). The dynamin-related *E. coli* protein YjdA (J05620) was used as outgroup. These sequences were aligned using the ClustalX package, and the phylogenetic tree was calculated by the N-J method in PAUP (34). The bootstrap values based on 1,000 replicates are shown.

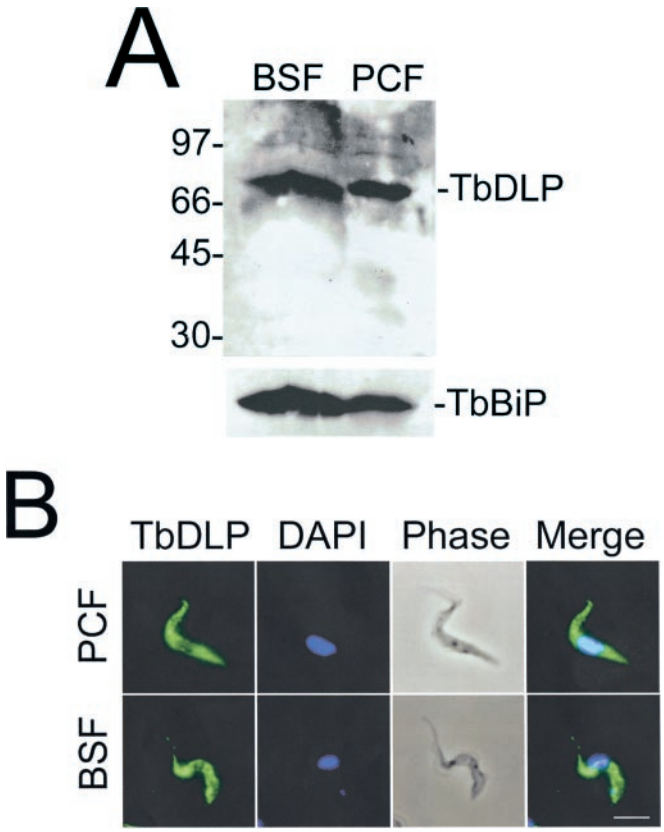

FIG. 2. **Characterization of antibodies against TbDLP.** *A*, protein extracts from BSF and PCF analyzed by Western blotting with anti-TbDLP. Trypanosomal binding protein (*TbBiP*) is used as a loading control. *B*, immunofluorescence images of PCF and BSF cells stained with antibodies against TbDLP show TbDLP is located at punctate structures distributed throughout the cell. The cells were also stained with DAPI to identify the nucleus and the kinetoplast. The corresponding phase image is shown, and merged images of the TbDLP stain and DAPI fluorescence are shown at right. *Scale bar*, 5 μm.

to assign the compartments to which the protein is targeting, we performed indirect immunofluorescence co-localization studies with markers shown previously to label sites of dynamin and dynamin-like protein action. These are as follows: the mitochondrion, the sites of release of CCVs, the ER, and glycosomes (Fig. 3*A*). We selected the PCF stage for this analysis because this stage has a more developed mitochondrion. To stain the mitochondria, wild type procyclic form cells were labeled with MitoTracker Red CMXRos prior to fixation and co-stained with anti-TbDLP antibodies. The punctate structures at the cell cortex labeled by TbDLP antibodies (*green*) partly co-localized with the mitochondrial network (*red*). This distribution is similar to that shown previously for yeast Dnm1p, which does not localize to the entire mitochondria outer membrane but assembles at discrete patches, appearing as rings that wrap around a mitochondrion or as clusters located on one side of a mitochondrial tube (40). To investigate potential TbDLP function in clathrin-mediated transport from the *trans*-Golgi network and/or endocytosis, PCF cells were also co-stained with a marker of the trypanosomal Golgi apparatus, TbRAB 31 (41), and trypanosomal clathrin heavy chain (27). Neither of these stains exhibited significant co-localization with TbDLP, suggesting that TbDLP is unlikely to function in CCV biogenesis.

The mammalian dynamin-like protein DLP1 is required for normal distribution and morphology of the endoplasmic reticulum, as well as the mitochondria. To examine if TbDLP performs a similar role in the maintenance of the ER in trypanosomes, co-localization studies were performed with TbBiP, an ER resident protein (39). TbDLP is found in regions of the cytoplasm adjacent to the ER, but little co-localization is observed in the merged panel (Fig. 3*A*). The proximity of the mitochondria to the ER has been observed previously in other systems and may be a consequence of Ca^{2+} exchange between the two organelles (43). A similar transfer may occur in *T. brucei* PCF where the mitochondrion volume is estimated at 25% of the total cell volume (44).

Recently, Vps1p has also been implicated in peroxisome abundance and inheritance (19). The kinetoplastid protozoa confine large parts of glycolysis within glycosomes, which are microbodies related to peroxisomes (45). To investigate the putative association of TbDLP with glycosomes, we performed co-localization studies with TbDLP and glyceraldehyde-3-phosphate dehydrogenase (GAPDH), a marker of glycosomes in *T. brucei* (45). We observed a very low degree of co-localization between TbDLP and TbGAPDH (Fig. 3*A*), and any overlap is probably a result of the extensive distribution of the mitochondrion. Similar staining patterns were observed for the tested markers in bloodstream form cells, but less mitochondrial signal was observed due to reduced mitochondrial function in this life stage (data not shown) (7).

To confirm the localization of TbDLP to the mitochondria, immunoelectron microscopy was performed. As described previously (21) the expected site of a dynamin-like protein involved in mitochondrial division would be at sites preparing to divide, sites actively dividing (appearing as constrictions of the mitochondria), and mitochondrial tips. Immunoelectron microscopy using TbDLP antiserum shows the protein has a similar distribution to that observed for yeast DNM1p, as it is localized to the mitochondrion membrane (21) (Fig. 3*B*). Localization of TbDLP confirms the phylogenetic assignation of TbDLP as functioning in mitochondrial dynamics.

TbDLP Is Required for Maintenance of Mitochondrial Morphology—We next used RNA interference (RNAi), a powerful technique for assessing gene function in trypanosomes by gene-specific suppression of mRNA levels (46). This was performed using an integrated expression vector containing a fragment of the *TbDLP* gene under control of a tetracycline-inducible PARP promoter (35). Using the RNAit algorithm the TbDLP fragment used is predicted unlikely to co-suppress other transcripts (47). Induction of RNAi in 29-13 PCF cell line (30), by addition of tetracycline, led to a severe growth defect (Fig. 4*A*). The level of TbDLP protein decreased after induction of RNAi, and suppression was maximal at day 4, as shown by Western blotting (Fig. 4*B*). Equivalence of loading was confirmed by reprobing the filter with antiserum against β-tubulin. The growth defect appeared very rapidly, becoming apparent by day 1 when protein levels were down to ~40% of endogenous wild type levels. These observations suggest TbDLP protein has a half-life of approximately 2 days, and wild type levels are required for efficient protein function. A similar but more rapid reduction of TbDLP protein and suppression of growth was observed in the BSF (data not shown). No alterations to replication rate were seen when wild type PCF cells were grown in the presence of tetracycline.[2]

The role of TbDLP in the maintenance of the normal morphology of the *T. brucei* mitochondrion was assessed following RNAi by live cell fluorescence imaging using MitoTracker Green FM. Wild type PCF trypanosomes have a single mitochondrion that runs the length of the cell (Fig. 5, *top panel*). In the uninduced PCF p2T7^{Ti}/*DLP* the mitochondrion appears normal and is essentially indistinguishable from the parental

[2] C. L. Allen and M. C. Field, unpublished data.

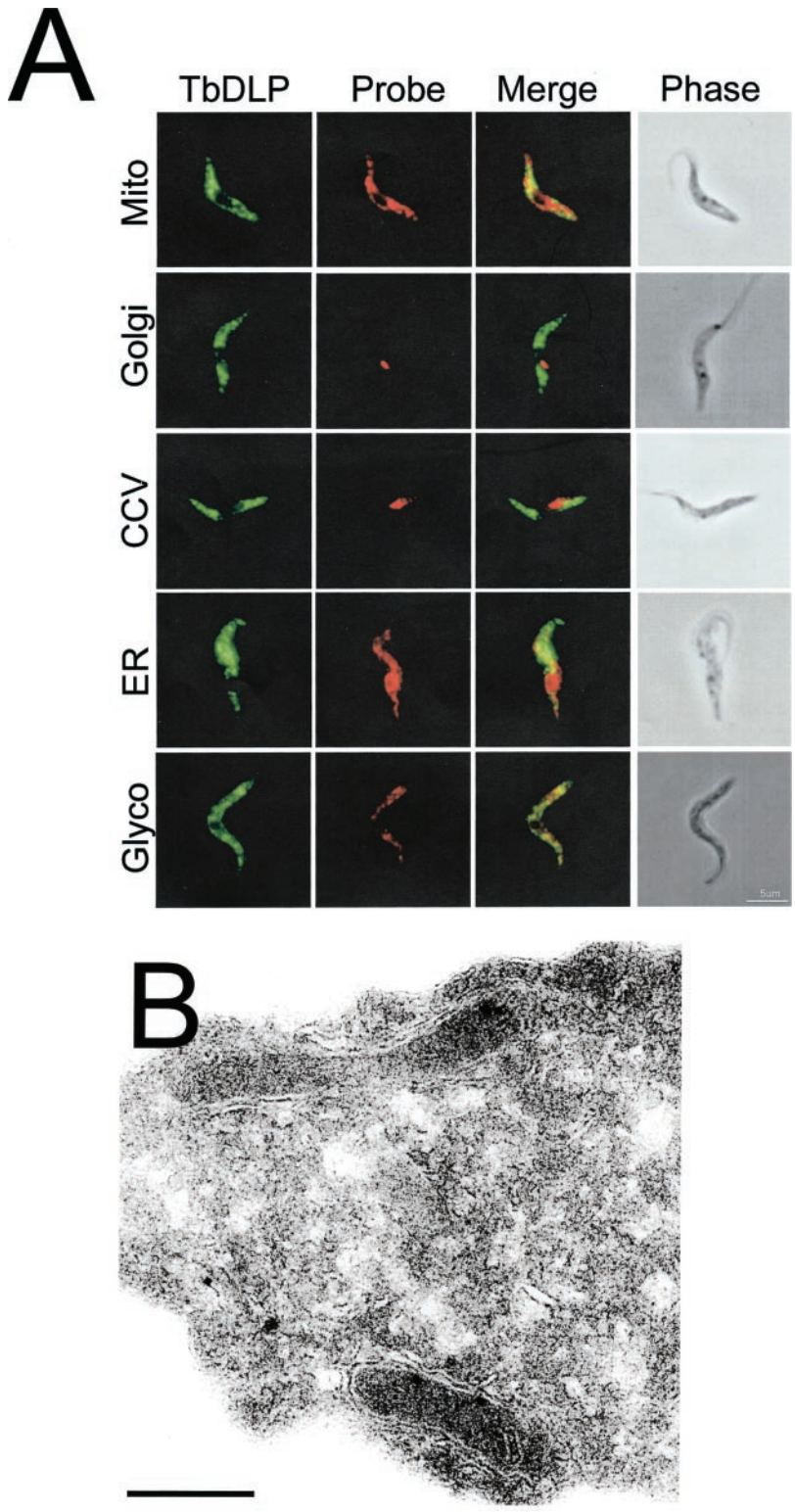

FIG. 3. **TbDLP is localized to the trypanosomal mitochondria.** *A*, immunofluorescence gallery of wild type PCF trypanosomes labeled with antibodies to TbDLP and various second markers for intracellular compartments. TbDLP fluorescence is shown at *left* in *green*, and the *second label left of center* in *red* (*Probe*). *Mito*, MitoTracker Red CMXRos was used to stain live cells prior to fixation. *Golgi*, antibodies against TbRab31; *CCV*, antibody to TbCHC; *ER*, antibody to TbBiP; and glycosomes (*Glyco*), antibody to TbGAPDH. All cells were counterstained with antibodies to TbDLP. Merged fluorescence images are shown at *right center*, and the corresponding phase images at *far left*. *Scale bar*, 5 μm. *B*, to confirm the localization of TbDLP to the mitochondria, immunoelectron microscopy was performed. TbDLP immunoreactivity is localized to the mitochondrion. *Scale bar*, 200 nm.

cell line. These data also confirm that the RNAi construct is not leaky. However, in live PCFs cells with depleted TbDLP, the extended mitochondrion observed in wild type cells has fused and collapsed into thick tubules, although the overall cell morphology appeared essentially unaltered by phase contrast imaging (Fig. 5, *lower panels*). Again, no alterations were seen in wild type PCFs exposed to tetracycline (data not shown). This phenotype is similar to that observed for yeast DNM loss of function mutants in which mitochondrial fission is abolished while fusion continues, thus resulting in the formation of elaborate net-like structures (20, 21). However, in this case the morphological effect is more complex as additional constriction points are also seen. This may reflect the fact that TbDLP is the only DLP in trypanosomes.

Analysis of TbDLP Silencing by Electron Microscopy—To confirm that mitochondrial distribution and morphology were altered by TbDLP RNAi, transmission electron microscopy was performed. In the uninduced cells, mitochondrial tubules appear as extended branched profiles distributed evenly in the peripheral cytoplasm, containing distinct cristae (invagina-

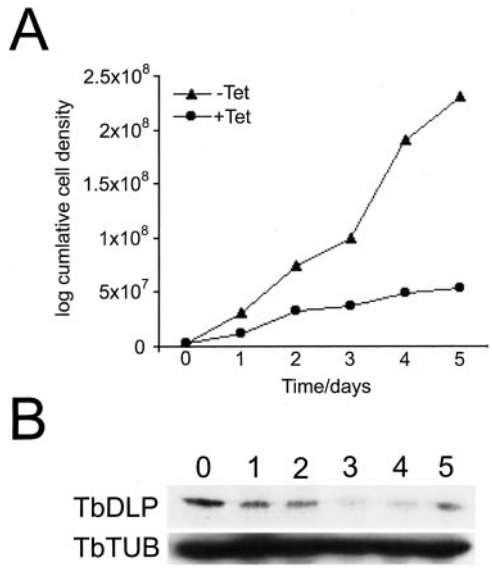

FIG. 4. **Silencing of TbDLP reduces trypanosome growth.** RNAi was induced in procyclic TbDLP cells by the addition of 1 μg/ml tetracycline. Cells were counted and diluted daily. *A*, cumulative growth curve with (*circles*) and without tetracycline (*triangles*). *B*, Western analysis of induced and uninduced cells using anti-TbDLP antiserum. Each lane was loaded with 15 μg of total cell protein, and β-tubulin was also used as a loading control.

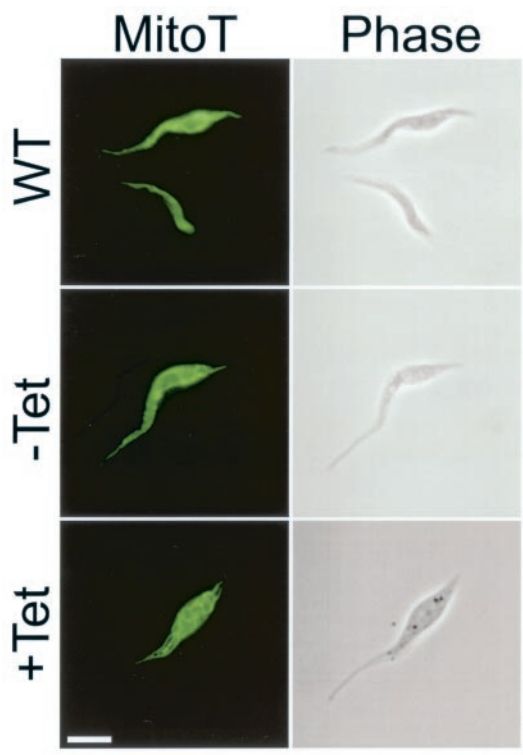

FIG. 5. **RNAi of TbDLP expression leads to mitochondrial abnormalities.** The mitochondria of wild type PCF (*WT*), uninduced PCF p2T7^{Ti}/*DLP* (−*Tet*), and PCF p2T7^{Ti}/*DLP* cells induced for 4 days (+*Tet*) were visualized using MitoTracker Green FM (*MitoT*) and live cell imaging. The corresponding phase image is shown at *right*. *Scale bar,* 5 μm.

tions of the inner mitochondrial membrane) (Fig. 6*A*). The mitochondrial genome, the kinetoplast, is also visible in this section. In the mitochondrion of p2T7^{Ti}/*DLP* cells induced for 4 days, normal cristae are present, but increased number of mitochondrial constrictions was seen (Fig. 6*B, arrowheads*). The ER is also visible in Fig. 6*D*, and this appears unaltered by TbDLP silencing. A higher magnification of a constricted mitochondrial profile is shown in Fig. 6*C*. These mitochondrial tubules were usually interconnected or branched, indicating that p2T7^{Ti}/*DLP* mitochondrial membranes still retain some features of a mitochondrial network. However, in some cells the network collapses into a flattened sheet with a series of fenestrations (marked by an *asterisk* in Fig. 6*D*). These data confirm that suppression of TbDLP has clear effects on the trypanosome mitochondrion and that TbDLP functions in the latter steps of mitochondrial division.

TbDLP RNAi Silencing Does Not Affect the Distribution of Other Organelles—To confirm TbDLP functions principally in the maintenance of mitochondrial morphology, we investigated the effect of TbDLP silencing on the morphology and distribution on other organelles using immunofluorescence analysis. The distribution of markers of the Golgi complex (TbRab31), clathrin coats (TbCHC), the endoplasmic reticulum (TbBiP), and glycosomes (TbGAPDH) appears to be essentially unaffected under RNAi relative to the wild type appearance (Fig. 7). Staining with DAPI indicates the distribution of the nucleus and kinetoplast appears normal; although repression of TbDLP resulted in abnormal mitochondrial membrane morphology, the mitochondrion retained the kinetoplast nucleoid. No evidence for abnormal cell cycle segregation of the kinetoplast was observed (data not shown); therefore, TbDLP is unlikely to be involved in mitotic segregation of kinetoplast DNA.

TbDLP Has No Detectable Role in Endocytosis—A number of the dynamin family proteins have an important role in membrane transport, particularly in endocytosis. *T. brucei* has a highly active endocytic system that appears to be essential (28). To investigate any potential role for TbDLP in endocytosis, we analyzed the internalization and trafficking of ConA in parental and TbDLP-silenced bloodstream form parasites, the stage with the most active endocytic system. ConA is an excellent marker for the endocytosis of membrane-bound ligands from the flagellar pocket (27, 37). Uninduced and induced p2T7^{Ti}/*DLP* cells were incubated with fluorescein isothiocyanate-ConA at 4 °C for 30 min to allow ConA to bind to high mannose containing determinants on the cell surface; the cells were washed to remove excess ConA and then warmed to 37 °C. The internalization of ConA over a 40-min period was monitored. The kinetics of ConA internalization in uninduced and induced cells were identical (Fig. 8). At time 0, all ConA is associated with the cell surface, but following 10 min at 37 °C, ConA is visible on the plasma membrane and also is enriched in vesicular structures near the flagellar pocket. At 20 min the majority of the ConA is present in intracellular pools with decreased staining of the cell surface. By 30 and 40 min the vast majority of the ConA has moved further into the cell and is present in large vesicular structures typical of lysosomes (27, 37). The finding that the kinetics of ConA uptake in cells subject to TbDLP RNAi are indistinguishable from uninduced cells indicates that TbDLP has no major role in endocytosis or transport within the endosomal pathway.

DISCUSSION

Mitochondria are presumed to derive from endosymbiont α-proteobacteria (48). During the course of evolution, the ancient mitochondria divided using a matrix-localized, α-proteobacterial type FtsZ protein and other bacterial type components. FtsZ assembles into a cytoskeletal framework associated with the cytoplasmic membrane at the division site and appears to play the major role in constriction of the furrow at septation in prokaryotes. FtsZ also functions in chloroplast division (49). There is no *FtsZ* in the completed genomes of *S. cerevisiae* and *C. elegans* where it appears FtsZ function has

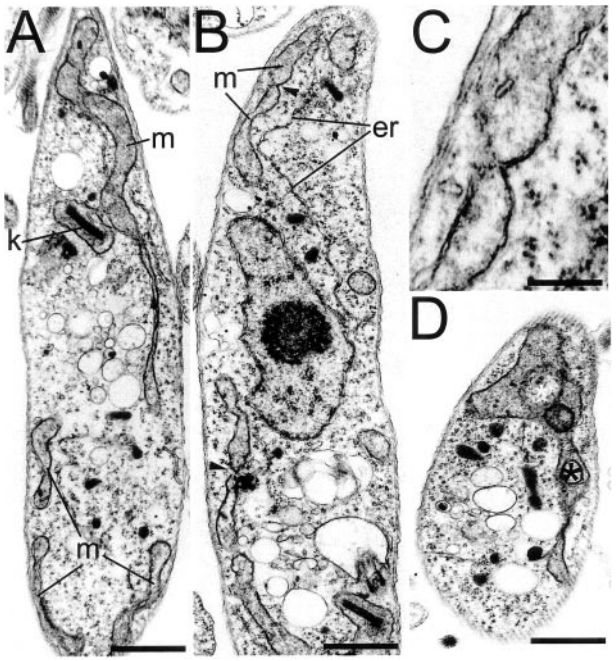

FIG. 6. **Electron microscopy of TbDLP RNAi shows mitochondrial constriction and net formation.** Induced or uninduced p2T7^{Ti}/*DLP* PCF cells were fixed and processed for thin section transmission electron microscopy. *A*, in the uninduced cells mitochondrial (*m*) profiles appear as extended unbranched tubules distributed evenly in the peripheral cytoplasm containing distinct cristae. The kinetoplast (*k*) is also visible in this section. *B*, sections through p2T7^{Ti}/*DLP* cells induced for 4 days show mitochondria containing normal cristae, but the compartments often appear as a series of large constricted tubules. *er*, endoplasmic reticulum. *C*, a higher magnification of the site of a constriction is shown. *Arrowheads* indicate sites of constriction. *D*, in some cells the network collapses into a flattened sheet with a series of fenestrations marked by an *asterisk*. *Scale bars* for *A*, *B*, and *D*, 1 μm; *C*, 0.3 μm.

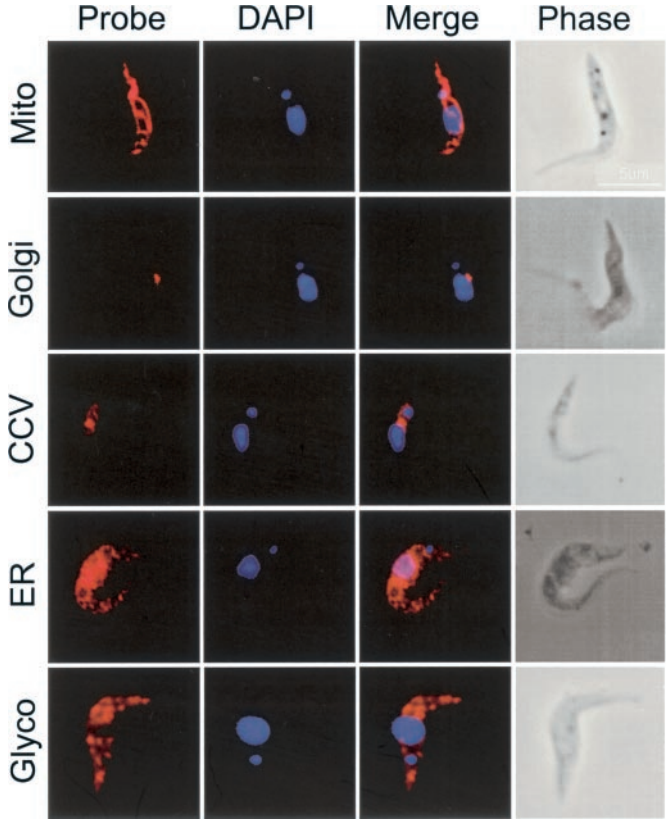

FIG. 7. **Silencing of TbDLP does not affect the morphology or distribution of other organelles.** Immunofluorescence gallery of induced p2T7^{Ti}/*DLP* PCF trypanosomes labeled for various intracellular compartments. Probe is the fluorophore and is shown in *red* at *left*. *Mito*, MitoTracker Red CMXRos was used to stain live cells prior to fixation. *Golgi*, antibodies against TbRab31; *CCV*, antibody to TbCHC; *ER*, antibody to TbBiP; and glycosomes (*Glyco*), antibody to TbGAPDH. All cells were counterstained with DAPI. Merged fluorescence images are shown at *right center* and the corresponding phase images at *far left*. *Scale bar*, 5 μm. Note that the mitochondrion has the collapsed tubular appearance but retains the kinetoplast DNA.

been superseded by the dynamin-like protein DNM (50). A *FtsZ* most closely related to the *FtsZ* of proteobacteria has been identified in the golden-brown alga *Mallomonas splendens* (51), and recently, the red alga *C. merolae* has been shown to retain a Ftz-based mitochondrial division ring but also uses a dynamin-like protein in the final mitochondrial severance (52). *C. merolae* has only two dynamin family proteins, the second DLP (CmDnm2) localizes at the chloroplast division site, showing a mechanism common to chloroplast and mitochondrial division (53).

The kinetoplastida are the earliest diverging eukaryotic groups that contain a single mitochondrion, and these studies establish TbDLP as an important regulator of mitochondrial morphology. The dynamin superfamily is subdivided into several groups, each named after the prototypic member: dynamin, DNM/VPS1, Mx, Mgm1p, and plant DLPs involved in plate formation and vesicular trafficking (17). By using phylogenetic analyses, TbDLP segregates into the large clade of DLPs that function primarily in mitochondrial division. The high degree of functional and sequence similarity among lower and higher eukaryotic dynamins involved in mitochondrial division suggests DLPs originally evolved to perform this function. *T. brucei* is highly unusual in possessing only one dynamin-like protein, which may represent a progenitor DLP.

The immunolocalization of TbDLP is consistent with the protein functioning in regulating the shape and distribution of the mitochondrion. TbDLP is localized to punctate structures on the mitochondria by immunofluorescence and using immuno-EM where it is observed on mitochondrial membranes. *TbDLP* RNAi silencing results in mitochondrial membrane fusion, presumably as a result in the failure to complete mitochondrial division. In contrast to the extensive effects on mitochondrial morphology, no effect was observed on endocytosis or on the distribution of other organelles including the nucleus, kinetoplast, ER, Golgi complex, or glycosomes. Furthermore, TbDLP is unlikely to function in endocytosis as we observed no enlargement of the flagellar pocket as has been demonstrated previously in clathrin heavy chain mutants that are defective in endocytosis (28). Mitochondrial fusion and formation of mitochondrial nets have been observed previously in DNM mutants in yeast and worms (20, 21, 54).

A role for TbDLP in control of scission of the mitochondrial membrane is supported by ultrastructural analysis; in the absence of TbDLP, an increased prevalence of sites of mitochondrial constriction is observed. These constrictions indicate that *T. brucei* possesses the machinery for constricting the mitochondria membrane in the absence of either the mechanoenzymatic force or the GTPase effector function of TbDLP, which is required to ensure division. In other systems, division of the inner and outer mitochondrial membrane appears coordinated. In the muscle cells of the DRP-1 *C. elegans* mutant division of the mitochondrial inner membrane still occurs when division of the outer membrane was blocked (54), indicating animal mitochondria possess a separate inner membrane division mechanism that acts in concert with the external DRP complex. Our observations confirm *T. brucei* has a mechanism for division of the mitochondrial membrane and are consistent

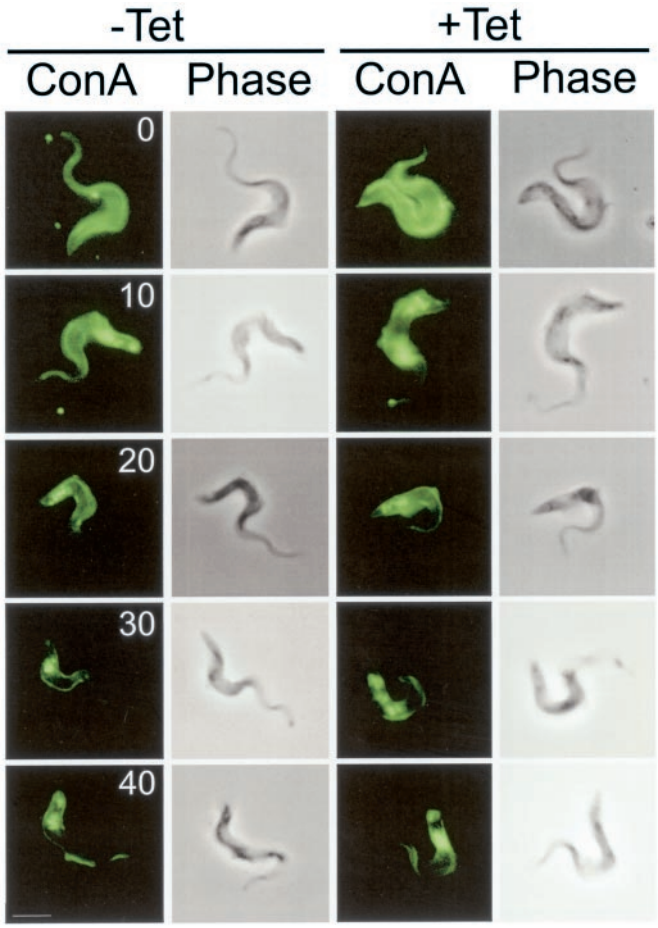

FIG. 8. **Endocytosis of ConA occurs with wild type kinetics in TbDLP RNAi mutants.** Bloodstream form p2T7^{Ti}/*DLP* cells were grown in the absence (−*Tet*) or presence (+*Tet*) of 1 μg/ml tetracycline for 4 days. Cells were labeled with ConA for 30 min at 4 °C, washed, and chased in fresh medium at 37 °C for up to 40 min. Aliquots removed at 0, 10, 20, 30, and 40 min and processed for fluorescence analysis. Representative fluorescence images and phase images are shown. *Scale bar,* 5 μm.

with TbDLP functioning as a regulator of the later stages of mitochondrial fission.

The abnormal mitochondria resulting from TbDLP silencing are efficiently partitioned during cell division and retain the kinetoplast. However, unlike ScDnm1p mutants (20), silencing of TbDLP RNAi results in a profound reduction of growth rate. The growth defect observed may arise because TbDLP has an addition function or may be because yeast has two cytoplasmic dynamins that may operate with a degree of functional redundancy. Alternatively, the defects observed here may restrict growth rate because of the more complex organization/partitioning of the trypanosomal mitochondria and the presence of addition trypanosomal cell cycle checkpoints.

The finding that TbDLP functions in mitochondrial membrane dynamics, coupled with the presence of a single dynamin family gene in trypanosomes, has clear implications for vesicle transport in these organisms and suggests that in kinetoplastids dynamins are not required in the endomembrane system. No ultrastructural evidence for dynamin collars on CCVs or pits has been obtained (55), and the finding that ConA endocytosis is unaltered by TbDLP suppression is consistent with this hypothesis. Hence, it appears that the original role of dynamin family proteins was in mitochondrial and chloroplast membrane scission, and that the endocytic and exocytic functions for dynamin have arisen later in evolution. Taken together these results indicate TbDLP has a very specific role in defining the shape and distribution of the mitochondrial network. This study adds to our understanding of the molecular mechanism and the evolutionary processes that underlie the division of organelles.

Acknowledgments—We are grateful to George Cross (Rockefeller University) for inducible cell lines, Jay Bangs (University of Wisconsin) for antibodies to TbBiP, and Paul Michels (Catholic University of Louvain) for antibodies to GAPDH. We also thank Clare Allen for data showing a lack of influence of tetracycline on growth of PCFs. Sequence data used in identifying and characterizing TbDLP homologues were obtained from The Wellcome Trust Sanger Institute and the Institute for Genomic Research *T. brucei* genome projects, and this is gratefully acknowledged.

REFERENCES

1. Sogin, M. L., and Silberman, J. D. (1998) *Int. J. Parasitol.* **28,** 11–20
2. Chen, J., Rauch, C. A., White, J. H., Englund, P. T., and Cozzarelli, N. R. (1995) *Cell* **80,** 61–69
3. Robinson, D. R., and Gull, K. (1991) *Nature* **352,** 731–733
4. Ogbadoyi, E. O., Robinson, D. R., and Gull, K. (2003) *Mol. Biol. Cell* **14,** 1769–1779
5. Matthews, K. R. (1999) *Parasitol. Today* **15,** 76–80
6. Morgan, G. W., Hall, B. S., Denny, P. W., Field, M. C., and Carrington, M. (2002) *Trends Parasitol.* **18,** 540–546
7. Priest, J. W., and Hajduk, S. L. (1994) *J. Bioenerg. Biomembr.* **26,** 179–191
8. Vickerman, K. (1965) *Nature* **208,** 762–766
9. Vickerman, K. (1985) *Br. Med. Bull.* **41,** 105–114
10. van der Bliek, A. M., and Meyerowitz, E. M. (1991) *Nature* **351,** 411–414
11. Hinshaw, J. E. (2000) *Annu. Rev. Cell Dev. Biol.* **16,** 483–519
12. Obar, R. A., Collins, C. A., Hammarback, J. A., Shpetner, H. S., and Vallee, R. B. (1990) *Nature* **347,** 256–261
13. Gibson, T. J., Hyvonen, M., Musacchio, A., Saraste, M., and Birney, E. (1994) *Trends Biochem. Sci.* **9,** 349–353
14. Warnock, D. E., Hinshaw, J. E., and Schmid, S. L. (1996) *J. Biol. Chem.* **271,** 22310–22314
15. Warnock, D. E., Terlecky, L. J., and Schmid, S. L. (1995) *EMBO J.* **14,** 1322–1328
16. Danino, D., and Hinshaw, J. E. (2001) *Curr. Opin. Cell Biol.* **13,** 454–460
17. van der Bliek, A. M. (1999) *Trends Cell Biol.* **9,** 96–102
18. Vater, C. A., Raymond, C. K., Ekena, K., Howald-Stevenson, I., and Stevens, T. H. (1992) *J. Cell Biol.* **119,** 773–786
19. Hoepfner, D., van den Berg, M., Philippsen, P., Tabak, H. F., and Hettema, E. H. (2001) *J. Cell Biol.* **155,** 979–990
20. Otsuga, D., Keegan, B. R., Brisch, E., Thatcher, J. W., Hermann, G. J., Bleazard, W., and Shaw, J. M. (1998) *J. Cell Biol.* **143,** 333–349
21. Bleazard, W., McCaffery, J. M., King, E. J., Bale, S., Mozdy, A., Tieu, Q., Nunnari, J., and Shaw, J. M. (1999) *Nat. Cell Biol.* **5,** 298–304
22. Wong, E. D., Wagner, J. A., Gorsich, S. W., McCaffery, J. M., Shaw, J. M., and Nunnari, J. (2000) *J. Cell Biol.* **151,** 341–352
23. Song, B. D., and Schmid, S. L. (2003) *Biochemistry* **42,** 1369–1376
24. Sweitzer, S. M., and Hinshaw, J. E. (1998) *Cell* **93,** 1021–1029
25. Takei, K., Haucke, V., Slepnev, V., Farsad, K., Salazar, M., Chen, H., and De Camilli, P. (1998) *Cell* **94,** 131–141
26. Sever, S., Muhlberg, A. B., and Schmid, S. L. (1999) *Nature* **398,** 481–486
27. Morgan, G. W., Allen, C. L., Jeffries, T. R., Hollinshead, M., and Field, M. C. (2001) *J. Cell Sci.* **114,** 2605–2615
28. Allen, C. L., Goulding, D., and Field, M. C. (2003) *EMBO J.* **22,** 4991–5002
29. Field, H., and Field, M. C. (1997) *J. Biol. Chem.* **272,** 10498–10505
30. Wirtz, E., Leal, S., Ochatt, C., and Cross, G. A. (1999) *Mol. Biochem. Parasitol.* **99,** 89–101
31. Altschul, S. F., Gish, W., Miller, W., Myers, E. W., and Lipman, D. J. (1990) *J. Mol. Biol.* **215,** 403–410
32. Sambrook, J., Fritsch, E. F., and Maniatis, T. (1989) *Molecular Cloning: A Laboratory Manual,* Cold Spring Harbor Laboratory Press, Cold Spring Harbor, NY
33. Thompson, J. D., Gibson, T. J., Plewniak, F., Jeanmougin, F., and Higgins, D. G. (1997) *Nucleic Acids Res.* **25,** 4876–4882
34. Swofford, D. L. (1998) PAUP Version 4.0, Sinauer Associates, Inc., Sunderland, MA
35. LaCount, D. J., Bruse, S., Hill, K. L., and Donelson, J. E. (2000) *Mol. Biochem. Parasitol.*, **111,** 67–76
36. Harlow, E., and Lane, D. (1988) *Antibodies: A Laboratory Manual,* Cold Spring Harbor Laboratory Press, Cold Spring Harbor, NY
37. Brickman, M. J., Cook, J. M., and Balber, A. E. (1995) *J. Cell Sci.* **108,** 3611–3621
38. Wienke, D. C., Knetsch, M. L., Neuhaus, E. M., Reedy, M. C., and Manstein, D. J. (1999) *Mol. Biol. Cell* **10,** 225–243
39. Bangs, J. D., Uyetake, L., Brickman, M. J., Balber, A. E., and Boothroyd, J. C. (1993) *J. Cell Sci.* **105,** 1101–1113
40. Legesse-Miller, A., Massol, R. H., and Kirchhausen, T. (2003) *Mol. Biol. Cell* **14,** 1953–1963
41. Field, H., Sherwin, T., Smith, A. C., Gull, K., and Field, M. C. (2000) *Mol. Biochem. Parasitol.* **106,** 21–35
42. Pitts, K. R., Yoon, Y., Krueger, E. W., and McNiven, M. A. (1999) *Mol. Biol. Cell* **10,** 4403–4417
43. Berridge, M. J. (2002) *Cell Calcium* **32,** 235–249
44. Hecker, H. (1980) *Pathol. Res. Pract.* **166,** 203–217
45. Michels, P. A., Poliszczak, A., Osinga, K. A., Misset, O., Van Beeumen, J.,

Wierenga, R. K., Borst, P., and Opperdoes, F. R. (1986) *EMBO J.* **5,** 1049–1056
46. Ngo, H., Tschudi, C., Gull, K., and Ullu, E. (1999) *Proc. Natl. Acad. Sci. U. S. A.* **95,** 14687–14692
47. Redmond, S., Vadivelu, J., and Field, M. C. (2003) *Mol. Biochem. Parasitol.* **128,** 115–118
48. Lang, B. F., Gray, M. W., and Burger, G. (1999) *Annu. Rev. Genet.* **33,** 351–397
49. Osteryoung, K. W., Stokes, K. D., Rutherford, S. M., Percival, A. L., and Lee, W. Y. (1998) *Plant Cell* **10,** 1991–2004
50. Erickson, H. P. (2000) *J. Cell Biol.* **148,** 1103–1106
51. Beech, P. L., Nheu, T., Schultz, T., Herbert, S., Lithgow, T., Gilson, P. R., and McFadden, G. I. (2000) *Science* **287,** 1276–1279
52. Nishida, K., Takahara, M., Miyagishima, S. Y., Kuroiwa, H., Matsuzaki, M., and Kuroiwa, T. (2003) *Proc. Natl. Acad. Sci. U. S. A.* **100,** 2146–2151
53. Miyagishima, S. Y., Nishida, K., Mori, T., Matsuzaki, M., Higashiyama, T., Kuroiwa, H., and Kuroiwa, T. (2003) *Plant Cell* **15,** 655–665
54. Labrousse, A. M., Zappaterra, M. D., Rube, D. A., and van der Bliek, A. M. (1999) *Mol. Cell* **5,** 815–826
55. Grunfelder, C. G., Engstler, M., Weise, F., Schwarz, H., Stierhof, Y. D., Morgan, G. W., Field, M. C., and Overath, P. (2003) *Mol. Biol. Cell* **14,** 2029–2040